Supporting Information

Phadke et al. 10.1073/pnas.1201122109

SI Text

Monomer Synthesis and Characterization. Monomers *N*-acryloyl 2-glycine (A2AGA), *N*-acryloyl 4-aminobutyric acid (A4ABA), *N*-acryloyl 6-aminocaproic acid (A6ACA), *N*-acryloyl 8-aminocaprylic acid (A8ACA), and *N*-acryloyl 11-aminoundecanoic acid (A11AUA) were synthesized from glycine (Fisher Scientific, Inc.), 4-aminobutyric acid, 6-aminocaproic acid, 8-aminocaprylic acid (Acros Organics, Inc.), and 11-aminoundecanoic acid (Aldrich), respectively, as described elsewhere (1). Briefly, for A2AGA, 0.1-mol glycine and 0.11-mol NaOH were dissolved in 80 mL deionized water in ice bath under vigorous stirring. To this, 0.11-mol acryloyl chloride in 15 mL tetrahydrofuran was added dropwise. The pH was maintained at 7.5–7.8 until the reaction was complete. The reaction mixture was then extracted with ethyl acetate. The clear aqueous layer was acidified to pH 2.0 and then extracted again with ethyl acetate. The organic layers were collected, combined, and dried over sodium sulfate. The solution was then filtered, concentrated, and precipitated in petroleum ether. Further purification was achieved by repeated precipitation and the product was lyophilized. Synthesis of other monomers followed similar procedure, with variations in pH during the acidification: pH 2.0 for A4ABA, pH 3.0 for A6ACA, and pH 5.0 for A8ACA and A11AUA. Proton nuclear magnetic resonance spectra (^{1}H NMR) of monomers were recorded with a Varian Mercury-400 spectrometer at 400 MHz. Carbon-13 nuclear magnetic resonance spectra (^{13}C NMR) were recorded on a Varian Mercury-400 spectrometer at 100 MHz; $CDCl_3$ or D_2O were used as solvents (1).

Synthesis of Hydrogels. Hydrogels were prepared by free radical polymerization in aqueous solution containing 1 mmol/mL of monomer, *N*,*N*′-methylene bisacrylamide (Bis-Am), 0.5% ammonium persulfate (initiator), and 0.1% tetramethylethylenediamine (accelerator) (Fig. S1*A*). To synthesize A6ACA hydrogels containing different cross-linker content, 0.1%, 0.2%, and 0.5% (wt/vol) BisAm (Sigma-Aldrich, Inc.) was added to the 1 M deprotonated A6ACA solution and polymerized as described above using the ammonium persulfate/tetramethylethylenediamine (APS/TEMED) redox initiators for 16 h at 37 °C. To create hydrogels with varying pendant side chains, we followed the same procedure. Specifically, 1 M solutions of the respective monomers (0.1291 g/mL for A2AGA, 0.157 g/mL for A4ABA, 0.185 g/mL for A6ACA, 0.213 g/mL for A8ACA, and 0.241 g/mL for A11AUA) were deprotonated using equimolar NaOH and used.

Loosely cross-linked A6ACA hydrogels were prepared using high concentrations of A6ACA monomers via chain transfer (Fig. S1*B*). Previous studies have shown that alkyl monomers having long pendant side chains could lead to loosely cross-linked networks during radical polymerization as a consequence of chain transfer at high concentration of monomers (2). In this study, we adopted this concept to create loosely cross-linked A6ACA hydrogels, where 1 M A6ACA was dissolved in 1 M sodium hydroxide to deprotonate the carboxyl groups of A6ACA. This solution was then polymerized using 0.5% APS as initiator and 0.15% TEMED as accelerator in cylindrical polypropylene molds measuring 0.5 cm in diameter and 2.5 cm in length. Polymerization was allowed to proceed for 16 h at 37 °C. The as-synthesized hydrogels exhibited an intact swollen structure with an equilibrium swelling ratio of 56 ± 3 g/g in PBS (Fig. S2*A*).

The hydrogel formation was also characterized through ^{13}C NMR spectroscopy (Fig. S2*B*). The cross-linked hydrogels were dialyzed against deionized (DI) water in a dialysis tube [molecular weight cutoff (MWCO) = 500 Da] for 48 h and ground in a mortar into fine particles and then freeze-dried. The freeze-dried powder was swollen in D_2O for NMR analysis. Carbon-13 NMR spectroscopy was recorded on a Varian VX500 500 MHz spectrometer. The NMR spectrum was compared against linear A6ACA polymer as described below. Linear poly(*N*-acryloyl 6-aminocaproic acid) was dissolved in D_2O at a concentration of 1% (wt/vol); lightly cross-linked polyA6ACA was fully swollen in D_2O and transferred into an NMR tube before spectroscopic analysis. Fig. S2*B* shows that all peaks of the loosely cross-linked-A6ACA hydrogels (178.2, 36.1, 33.0, 24.9, 22.5, and 21.2 ppm) were identical or close to those in the spectrum of linear polyA6ACA except for one peak at 67.0 ppm (labeled by an asterisk). This additional peak is attributed to chemical cross-links formed during polymerization as a consequence of chain transfer at high monomer concentration (3, 4).

Synthesis of Linear A6ACA Polymer. Two grams (10.8 mmol) of A6ACA, 0.432 g (10.8 mmol) of NaOH, and 7.8 mg (0.1 mmol) of 2-mercaptoethanol (chain transfer agent) were dissolved in 40 mL of DI water at room temperature. Upon complete dissolution of the reactants, 40 μL of TEMED was added to the solution, and purged with argon for 30 min; 20 mg of APS in 2 mL of DI water was then added to the solution under argon purge. The solution was transferred to an oil bath at 40 °C and reacted overnight. The polymer solution was cooled to room temperature and poured into 800 mL of acetone. The precipitate was collected and dried under vacuum at room temperature. The product was further purified by dialysis against DI water in a dialysis tube (MWCO = 500 Da) for 48 h and freeze-dried before analysis. The usage of 2-mercaptoethanol as a chain transfer agent avoids the transfer of free radical to the polymer backbone and thereby prevents subsequent cross-linking of the polymer (3).

Hydrogel Swelling Ratio Measurements. The hydrogels were immersed in excess of 1× PBS (pH 7.4) for 48 h following synthesis to allow equilibration with constant change of PBS. The hydrogels were weighed after equilibrium swelling to determine their wet weight and after subsequent freeze-drying to determine their dry weight. Swelling ratio was calculated as the ratio of wet to dry weight. Samples were prepared as triplicates and averages were calculated with standard deviation (Fig. S2*C*).

Spectroscopic Analyses. Spectroscopic analysis was carried out on healed and unhealed A6ACA hydrogels. Samples were dried at 37 °C for 24 h prior to measurement of Raman and FTIR spectra. The Raman spectra of the healed and unhealed (samples are shown in Fig. 2*A*). The appearance of a band at 1,409 cm^{-1} for unhealed hydrogels indicates the presence of carboxylate (COO^-) functional groups. This frequency is well within the typical range expected for the COO^- symmetric stretch; the corresponding band in the FTIR spectrum is at 1,403 cm^{-1} (5, 6) (Fig. 2*B*). The healed samples uniquely exhibits a strong Raman band at 1,714 cm^{-1} (Fig. 2*A*), which is best assigned to a hydrogen-bonded carboxylic acid group. The corresponding band in the FTIR spectrum (Fig. 2*B*) is at 1,704 cm^{-1}. The close correspondence of the IR and Raman frequencies indicates that this pair of bands is unlikely to be a signature of a cyclic carboxylic acid dimer. A cyclic dimer generally has a Raman-active in-phase combination of C = O stretches that is expected to be downshifted to 1,680–1,640 cm^{-1} and an IR active out-of-phase combination located in the 1,720–1,680 cm^{-1} range (5). Furthermore, a cyclic

carboxylic acid dimer would be expected to show other signatures of out-of-plane OH···O hydrogen deformation in the 960–875 cm^{-1} region of the FTIR spectrum, and these bands are either weak or absent in healed protonated hydrogels (5). A reasonable hypothesis is that some of the protonated −COOH groups reach the amide groups of opposing pendant chains, and form a pair of H bonds (acceptor and donor) to the respective NH and C = O groups of the amide (interleaved configuration). The following spectral assignments are consistent with this configuration.

1. Raman and IR activity at 1,714/1,704 cm^{-1} is attributed to the C = O stretch of the carboxylic acid group that is hydrogen bonded to the NH of the amide.
2. The NH stretch at 3,310 cm^{-1} is a typical frequency for an H-bonded N-H group.
3. A prominent band in the healed A6ACA hydrogel FTIR spectrum at 1,627 cm^{-1} and a corresponding weak band in the Raman spectrum at 1,624 cm^{-1} are assigned to the amide I mode (majority C = O stretch, some C–N stretch). These frequencies are approximately 18 cm^{-1} downshifted relative to the 1,642–1,643 cm^{-1} band that is assigned to the amide I at high pH. A downshift is expected for enhanced H bonding to the amide group (5, 7) such as provided by direct interaction between −COOH and amide groups. A similar shift for A6ACA was noted in earlier work at pH 5.5; however, a spectrum at lower pH was not recorded and a strong band at 1,628 cm^{-1} was not clearly assigned to carboxylic acid/amide interaction as we propose here (5, 6).

We note substantial amide I band intensity at approximately 1,645 cm^{-1} (FTIR, shoulder) and 1,642 cm^{-1} (weak Raman band) for healed hydrogels, which is nearly the same frequency as the amide I in unhealed hydrogels (Fig. 2*A* and *B* and Table S1). This observation suggests that some population of amide groups has a similar H-bond environment at both pH extremes. For this population of interacting chains, the formation of interleaved pendant chains at low pH seems implausible. Instead, it is possible that some of the −COOH groups hydrogen bond with pairs of −COOH groups on opposing strands, in a manner that has previously been termed as "face-on" (7, 8). The amide groups of this subset of pendant chains would have similar interactions with each other (or with a neighboring water molecule) at either high or low pH, which is consistent with the similar amide I frequencies at low and high pH. Furthermore, the fact that the face-on structure is less symmetric than a cyclic dimer is consistent with the overlapping IR and Raman frequencies.

Molecular Dynamics Simulations of Hydrogel Networks To investigate the effect of side-chain length on healing efficiency, we performed molecular dynamics simulations of hydrogel networks built from A6ACA, A8ACA, and A11AUA monomers having side chains of lengths 5, 7, and 10 CH_2 groups, respectively. The 3D network structure of the hydrogel comprising of 20 monomers between each cross-link was assembled using the procedure of Jang et al. (9). Our simulation box (unit cell) had dimensions of approximately 9.2 × 6.4 × 6.4 nm, and it consisted of water molecules and a nine-arm network motif placed symmetrically inside the simulation box. This motif consisted of two four-arm crossed junctions connected along the *x* direction by a chain of 20 monomers, where each arm was a chain of 10 monomers (see Fig. 4*A*, *Left*). The motif was placed symmetrically inside the simulation box such that its arms in the *y* and *z* direction touched the faces of the simulation box, whereas there was a 0.5-nm gap on either sides of the two junctions in the *x* direction. The simulation box, when replicated in all directions through periodic boundary conditions (PBCs), yielded the desired hydrogel network shown in Fig. 4*B* (*Right*). Specifically, implementation of PBCs allowed us to covalently connect the eight-arm ends to their periodic images in the *y* and *z* direction, whereas the water filled gap in the $\pm x$ direction prevented continuity of the network along the *x* direction and allowed the creation of a hydrogel–water interface in between periodic images of the network.

Because of computational challenges, we are limited to examining high cross-link densities: The cross-links in our network are separated by 20 monomers-long chains, whereas those in the experimental system are more sparsely distributed (approximately 150 monomers apart from rough calculations). However, because the side chains still remain significantly smaller than the molecular pores in the network, the side-chain conformations and their accessibility for mediating external hydrogen bonds are not likely to be affected much by the larger cross-link density used in our simulations. Hence, our "compact" model of the hydrogel network might still yield quantitative information on the conformations of the side chains and their dependence on side-chain length.

The intramolecular and intermolecular interactions in our network were described using the ab initio-based polymer consistent force field (10). All simulations were performed using the large-scale atomic/molecular massively parallel simulator package (http://lammps.sandia.gov). We added approximately 6,000 water molecules, treated using the TIP3P model, into the unit cells constructed for the networks studied here. The resulting configurations were energy minimized, equilibrated for 50 ps in the constant-volume-temperature ensemble at 300 K, thermally annealed at 800 K for 40 ps, and then cooled back to 300 K. Further equilibration was performed in the constant-pressure-temperature ensemble at 300 K and 1 atm. The time step was taken as 0.25 fs in all simulations and a Nose–Hoover thermostat was employed to keep temperature constant. The final equilibrated density of equilibrated hydrogels at 300 K and 1 atm was calculated as 1.092 g/cm^3 for A6ACA, 1.0744 g/cm^3 for A8ACA, and 1.065 g/cm^3 for A11AUA.

To determine the accessibility of the carboxyl and amide groups of the network side chains for mediating hydrogen bonds, we picked five representative configurations of the network from 250-ps-long simulation runs. We quantified the accessibility of each group in terms of the number of hydrogen bonds it forms with the water molecules. We hypothesize that the accessibility of the functional groups for interacting with water molecules is a good measure for their accessibility for interacting with functional groups from the apposing hydrogel surface. The number of hydrogen bonds mediated by the amide and carboxylic groups of the chosen configurations were calculated by using University of California, San Francisco Chimera software (http://www.cgl.ucsf.edu/chimera) using a tolerance of 0.3 Å and 20° from the precise geometrical criteria for hydrogen bonding (11).

1. Ayala R, et al. (2011) Engineering the cell-material interface for controlling stem cell migration, adhesion and differentiation. *Biomaterials* 32:3700–3711.
2. Lazar M, Hrckova L, Fiedlerova A, Borsig E (2000) Cross-linking during radical polymerization of dodecyl methacrylate. *Macromol Mater Eng* 283:88–92.
3. Xu Y, Li G, Haraguchi K (2010) Gel formation and molecular characteristics of poly(N-isopropylacrylamide) prepared by free radical polymerization in aqueous solution. *Macromol Chem Phys* 211:977–987.
4. Britton D, Heatley F, Lovell PA (1998) Chain transfer to polymer in free-radical bulk and emulsion polymerization of vinyl acetate studied by NMR spectroscopy. *Macromolecules* 31:2828–2837.
5. Colthup NB, Daly LH, Wiberley SE (1975) *Introduction to Infrared and Raman Spectroscopy* (Academic, New York), pp 289–325.
6. Barbucci R, Casolaro M, Magnani A (1989) Vinyl polymers containing amido and carboxyl groups as side substituents. 2. Thermodynamic and fourier-transform infrared spectroscopic studies for the protonation of poly(N-acryloylglycine) and poly(N-acryloyl-6-aminocaproic acid). *Makromol Chem* 190:2627–2638.
7. Barth A, Zscherp C (2002) What vibrations tell us about proteins. *Quart Rev Biophys* 35:369–430.

8. Dong J, Ozaki Y, Nakashima K (1997) Infrared, Raman and near-infrared spectroscopic evidence for the coexistence of various hydrogen-bond forms in poly(acrylic acid). *Macromolecules* 30:1111–1117.
9. Jang SS, Lee SG, Brunello GF, Lee JH, Bucknall DG (2009) Effect of monomeric sequence on mechanical properties of p (VP-co-HEMA) hydrogels at low hydration. *J Phys Chem B* 113:6604–6612.
10. Sun H (1998) COMPASS: An ab initio force-field optimized for condensed-phase applications—overview with details on alkane and benzene compounds. *J Phys Chem B* 102:7338–7364.
11. Mills J, Dean PM (1996) Three-dimensional hydrogel-bonded geometry and probability information from a crystal survey. *J Comput Aided Mol Des* 10:607–622.

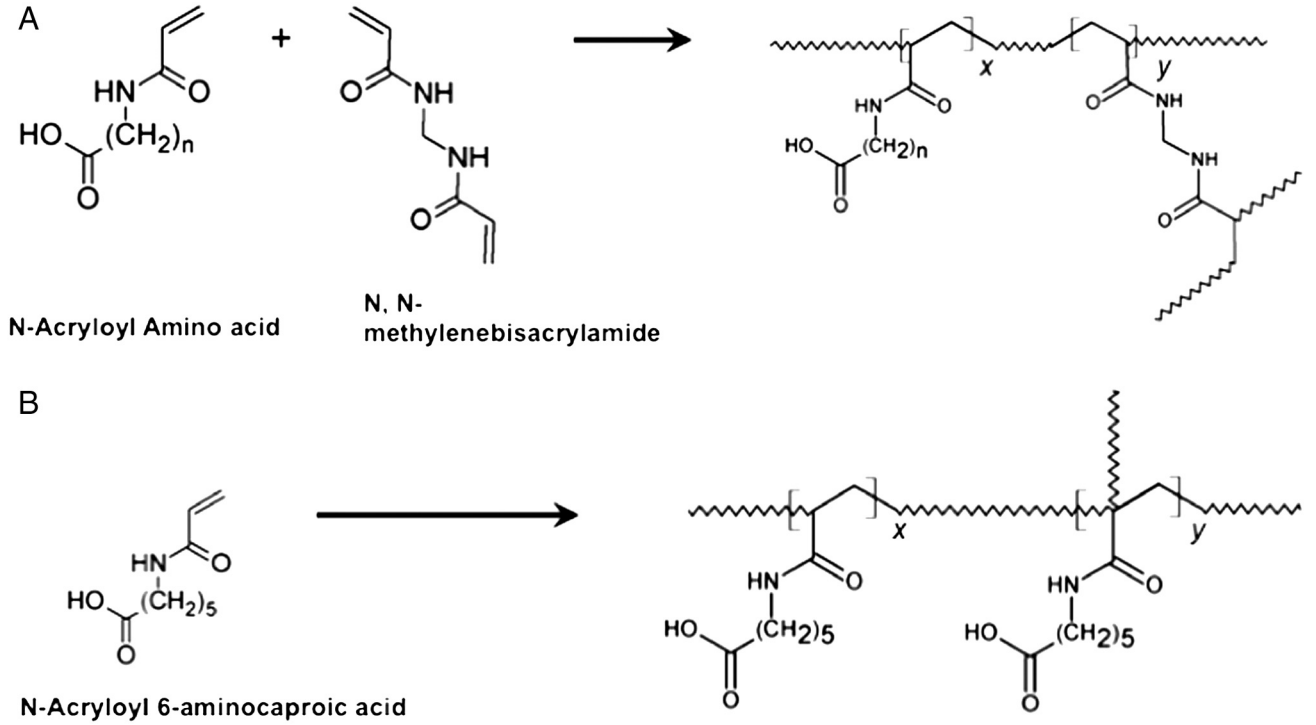

Fig. S1. Reaction scheme for the synthesis of hydrogels. (*A*) Synthesis of *N*-acryoloyl amino acid hydrogels with varying side-chain lengths (A2AGA, $n = 1$; A4ABA, $n = 3$; A6ACA, $n = 5$; A8ACA, $n = 7$; and A11AUA, $n = 10$) by using *N*,*N*′-methylenebisacrylamide as a cross-linker. (*B*) Loosely cross-linked *N*-acryloyl 6-aminocaproic acid in the absence of *N*,*N*′-methylenebisacrylamide. In both of the schemes, $x \gg y$.

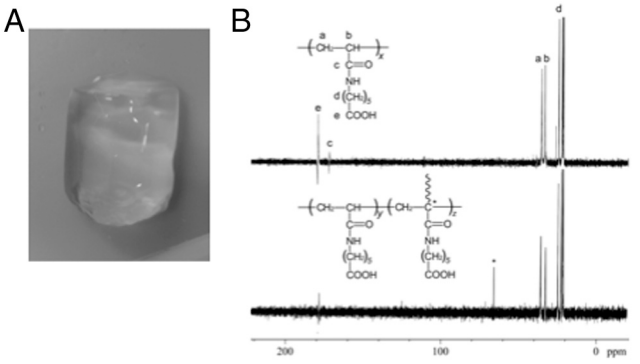

C

N,N'-methylene bisacrylamide content	Swelling ratio (gm/gm)
0%	56±3
0.1%	35±1
0.2%	29±2
0.5%	17±1

Fig. S2. Synthesis and characterization of A6ACA hydrogels. Equilibrium swollen, loosely cross-linked A6ACA hydrogel (*A*) and its ^{13}C NMR spectroscopic analysis (*B*). The top spectrum represents linear polyA6ACA, whereas the bottom spectrum represents the cross-linked A6ACA. All peaks of cross-linked A6ACA (178.2, 36.1, 33.0, 24.9, 22.5, and 21.2 ppm) are either identical or close to those of linear polymers, except for one peak at 67.0 ppm (labeled by the asterisk). This peak is attributed to chemical cross-links formed during the polymerization as a consequence of chain transfer at high monomer concentration. (*C*) Swelling ratio measurements for hydrogels synthesized with varying *N*,*N*′-methylenebisacrylamide content.

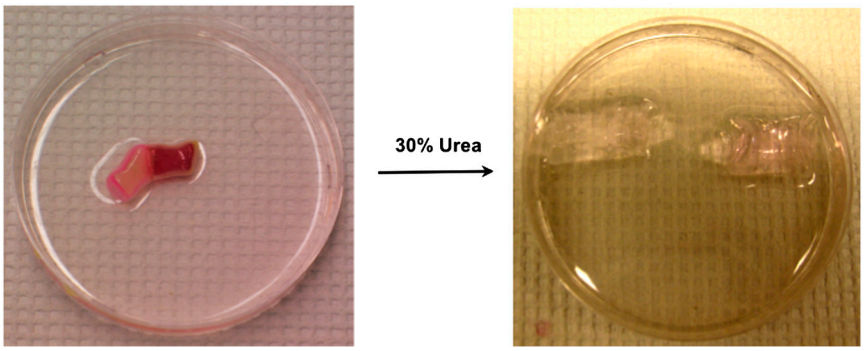

Fig. S3. Healed hydrogels (*Left*) separated upon exposure to 30% (wt/vol) solution of urea (*Right*).

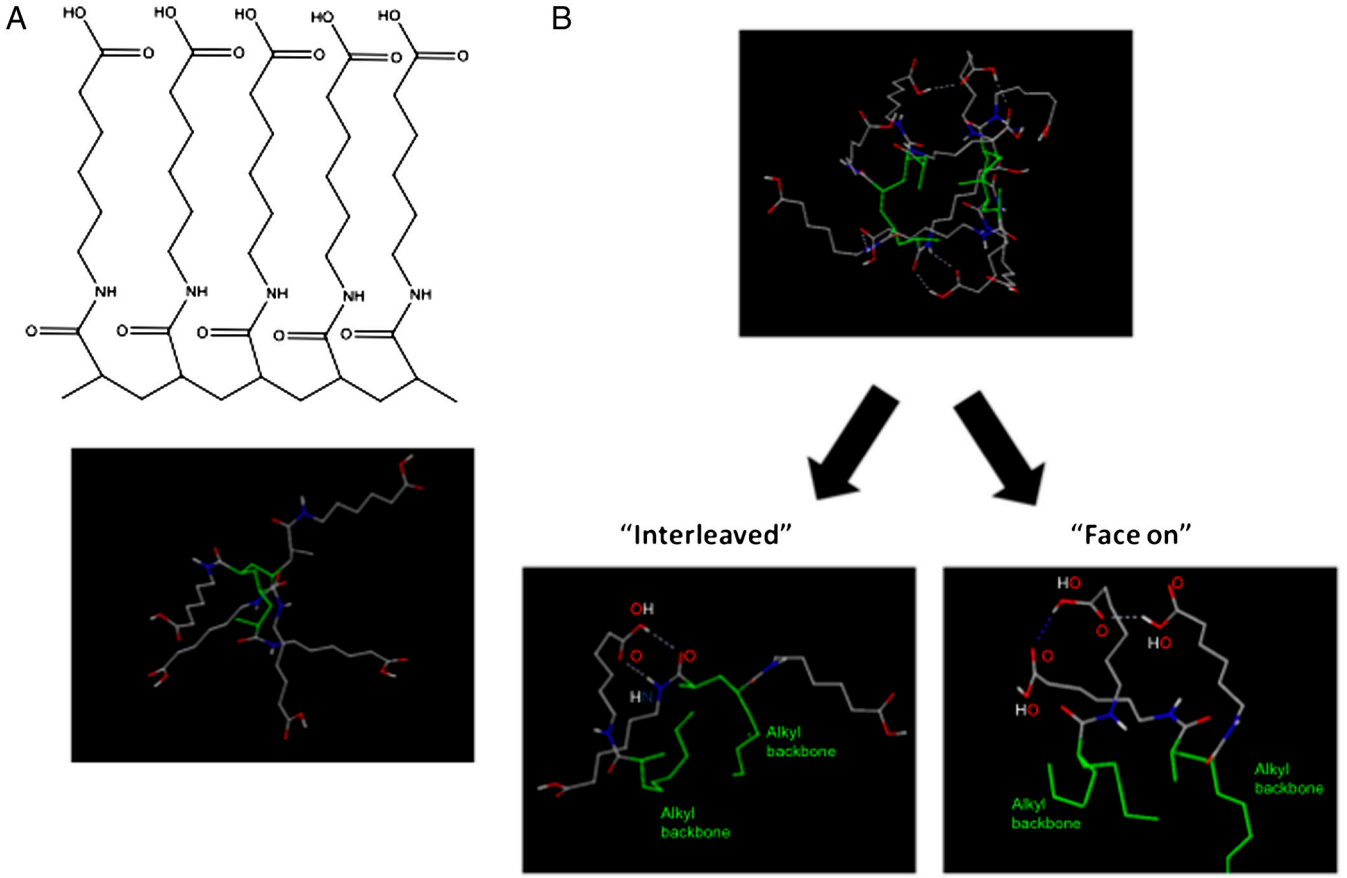

Fig. S4. Molecular modeling to determine steric feasibility of "interleaved" and "face-on" hydrogen bonding configurations of the pendant side chains. (*A*) Chemical structure of five-unit oligomer of A6ACA (*Top*) and its energy-minimized structure (*Bottom*). (*B*) The energy-minimized structure of two five-unit oligomers facing each other (*Top*) showing both interleaved (*Bottom*, *Left*) and face-on configurations (*Bottom*, *Right*). Dotted lines, intermolecular hydrogen bonds; green, alkyl backbone; gray, CH_2 groups in pendant side chain; blue, nitrogen; red, oxygen; and white, polar hydrogen.

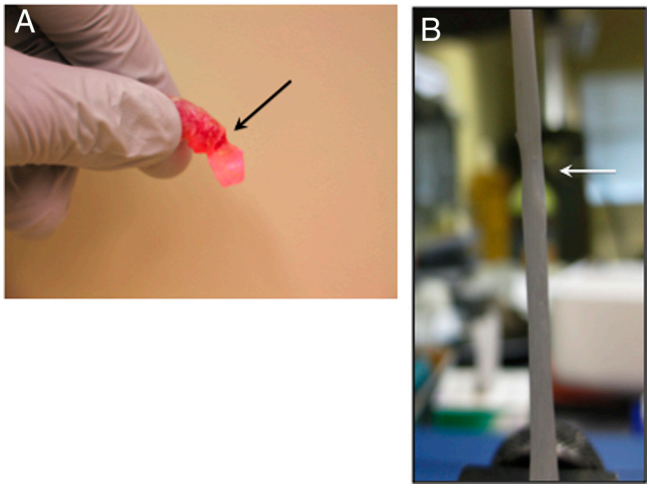

Fig. S5. (*A*) Hydrogels healed for 5 min fracture within the bulk region and not at the weld line. (*B*) Hydrogels healed for 24 h, which exhibit an opaque color, fracture at the weld line during tensile testing. The arrows indicate the weld line.

A

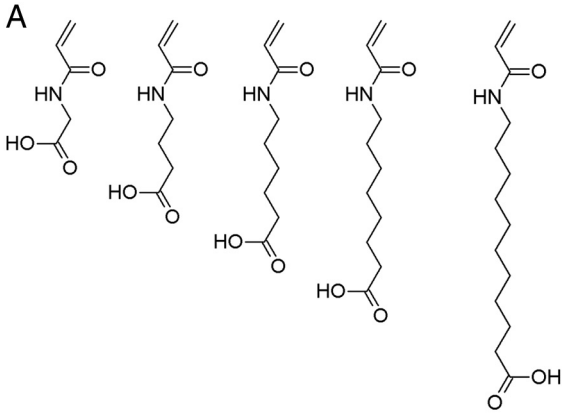

B

# of CH_2 in side chain	Healing
1	Did not heal
3	Did not heal
5	Strong, rapid healing
7	Weak, slow healing
10	Did not heal

Fig. S6. Effect of side-chain length on healing efficiency. (*A*) Chemical structure of *N*-acryloyl modified amino acids used to investigate the effect of side-chain length on healing ability (from left to right) *N*-acryloyl glycine (1 CH_2 group), *N*-acryloyl 4-aminobutyric acid (3 CH_2 groups), *N*-acryloyl 6- aminocaproic acid (5 CH_2 groups), *N*-acryloyl 8-aminocaprylic acid (7 CH_2 groups), and *N*-acryloyl 11-aminoundecanoic acid (10 CH_2 groups). (*B*) Table summarizing the effect of pendant side-chain length on healing.

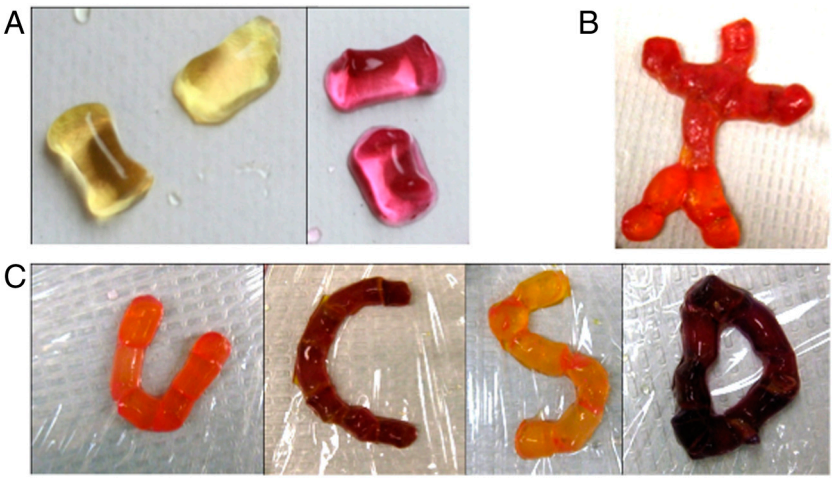

Fig. S7. A6ACA hydrogels fused to form complex architectures. (*A*) Unhealed cylindrical hydrogels, dyed maroon and yellow, respectively, and the same hydrogels healed to form a humanoid figure (*B*) and the letters "UCSD" (*C*). Yellow hydrogels were used to assemble the "U" and then separated by exposure to pH 13. They were then healed to form the "S." This procedure was repeated for "C" and "D," respectively. The differences in the order at which the four letters were assembled explains the differences observed in swelling and color.

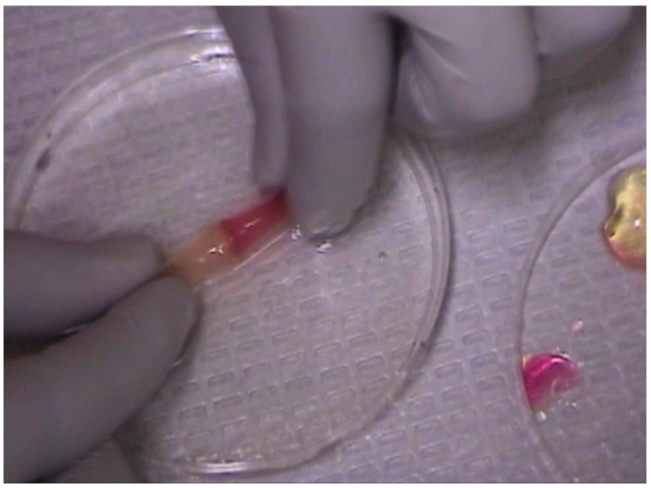

Movie S1. Healing of two hydrogel pieces in low-pH solution. The two pieces are dyed with colors for easy visualization.

Movie S1 (AVI)

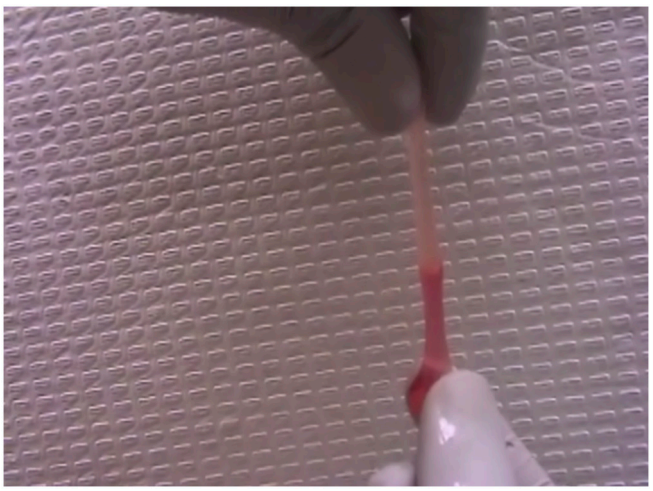

Movie S2. Strong weld-line strength of the healed hydrogels.

Movie S2 (AVI)

Table S1. Observed frequencies and assignments of infrared and Raman bands of healed and unhealed A6ACA hydrogels

Low pH		High pH		Assignments
Raman	IR	Raman	IR	
—	3,310	—	—	N–H stretch, H bonded (1, 2)
2,929, 2,866	2,925, 2,857	2,929, 2,866	2,930, 2,860	C–H stretches
—	2,500 (broad)	—	—	Overtone/combination bands (2)
1,714	1,704	—	—	C = O stretch of terminal carboxylic acid (2)
1,642	1,645	1,643	1,642	Amide I (1–3)
1,624	1,627	—	—	Amide I (H bonded to –COOH)
1,568	1,547	1,567	1,551	Amide II (2, 3); overlap with COO^- stretch (2) for high-pH IR
1,444	1,440	1,444	1,440	CH_2 bend deformation (2)
—	—	1,409	1,403	COO^- stretch (3)
1,355	1,386	—	—	OH deformation (2)
1,309, 1,265	—	1,309, 1,265	—	CH_2 wag or twist (4), and Amide III
—	1,271–1,192	—	—	C–O stretch coupled with C-O-H in-plane bend (2)
1,169–1,083	1,163–1,081	1,170–1,085	1,164–1,080	C-CH_2 and N-CH_2 stretches (4)
912–843	900 (broad)	947	860, 989	unassigned
—	—	561	—	COO^- rock

1. Roeges NPG (1994) *A Guide to the Complete Interpretation of Infrared Spectra of Organic Structures* (Wiley, New York).
2. Colthup NB, Daly LH, Wiberley SE (1975) *Introduction to Infrared and Raman Spectroscopy* (Academic, New York).
3. Barbucci R, Casolaro M, Magnani A (1989) Vinyl-polymers containing amido and carboxyl groups as side substituents. 2. Thermodynamic and Fourier-transform infrared spectroscopic studies for the protonation of poly(N-acryloylglycine) and poly(N-acryloyl-6-aminocaproic acid). *Makromol Chem* 190:2627–2638.
4. Dong J, Ozaki Y, Nakashima K (1997) Infrared, Raman, and near-infrared spectroscopic evidence for the coexistence of various hydrogen-bond forms in poly(acrylic acid). *Macromolecules* 30:1111–1117.

Table S2. Composition of buffers with varying pH

Buffer pH	Composition
1	27.17% 0.2 M potassium chloride + 72.83% 0.2 M hydrochloric acid
3	69.15% 0.1 M potassium hydrogen phthalate + 30.85% 0.1 M hydrochloric acid
4	99.8% 0.1 M potassium hydrogen phthalate + 0.02% 0.1 M hydrochloric acid
4.5	85.18% 0.1 M potassium hydrogen phthalate + 14.82% 0.1 M sodium hydroxide
5	68.87% potassium hydrogen phthalate + 31.13% 0.1 M sodium hydroxide